The Mid- to Late Pleistocene Ice Rafted Debris record at IODP Site 1308, Central North Atlantic

Research Thesis

Presented in Partial Fulfillment of the Requirements for graduation

"with Research Distinction in Earth Sciences" in the undergraduate colleges of

The Ohio State University

By

Colin Whyte

The Ohio State University

April 2014

Project Advisor: Professor Lawrence Krissek, School of Earth Sciences

Approved by

Lawrence A. Krissek, Advisor
School of Earth Sciences

TABLE OF CONTENTS

Abstract

Eighty-seven samples from cores recovered at Integrated Ocean Drilling Program Site 1308 in the central North Atlantic Ocean have been studied to create a record of ice-rafted debris (IRD) abundance and composition downcore, which was used to produce an IRD record through time. These samples span 525 ka to 853 ka and the record was compared with known marine isotope stages to see if any relationship exists between global climate state and ice-rafting at Site 1308. The lithologies of the individual grains in the terrigenous fraction were identified to determine the abundance of each grain type relative to total IRD. Some grain types are source area-specific, so compositional changes indicate changes in the relative importance of the IRD sources through time.

A count of 100 grains was made for each sample using a standardized counting technique and the grain types were identified and tallied. The percentages of terrigenous grains and biogenic grains were plotted vs. age as were the abundances of individual terrigenous grain types. The terrigenous fraction abundances show repeated fluctuations, with increases during the glacial marine isotope stages and near glacial-interglacial boundaries. The abundances of individual terrigenous grain types show similar increases during glacial stages and near glacial-interglacial boundaries, but none of the lithologic abundances follows exactly the same pattern as the total terrigenous fraction. Previous provenance studies determined that hematite-stained quartz, mafic rock fragments, and volcanic glass originated near the Gulf of St. Lawrence or southern Greenland, east central Greenland or Iceland, and Iceland, respectively. Variations in the abundances of these grains reveal frequent and often dramatic fluctuations in the relative rates of input from these IRD sources.

Acknowledgments

I would like to thank Dr. Larry Krissek for allowing me to be part of this ongoing research project and for his guidance throughout my research and especially during my data analysis.

I would also like to acknowledge the prior research on this project conducted by Michael Kellum that was used as a model for obtaining and analyzing the data.

A special thanks is given to Joel Main for his occasional Pandora Radio playing that was always very uplifting during research.

The cores were acquired as part of the Integrated Ocean Drilling Program, and samples were provided for undergraduate research by the Bremen Core Repository.

List of Figures

List of Tables

Introduction

As glaciers move across a landscape they erode and entrain rocks and sediment, which become embedded into the ice. When a glacier reaches a coastline it will extend out over the ocean until, under the proper conditions, ice calves creating icebergs. The sediment that was once trapped in the glacier is now trapped in the icebergs that drift with the ocean currents. The icebergs will drop this sediment to the seafloor as they melt generating ice-rafted debris (IRD), which builds a record of ice-influenced deposition on the seafloor. When combined with a dating method, such as biostratigraphy, magnetostratigraphy, and/or oxygen isotope stratigraphy, studying these sediments can define a record of IRD abundance variations through time, which can assist in identifying glacial fluctuations through time. In addition, IRD records can provide details on how individual iceberg source regions respond to glacial/interglacial changes, as some grain types in IRD are diagnostic of specific source areas. Determination of provenance can help describe the extent of glaciation in each source region, since the glaciers in an area must have reached the coastline in order to calve and create icebergs. The distribution of source-diagnostic grains can also be used to examine the behavior of ocean currents at the time of deposition.

This study examines sediment samples from core drilled by the Integrated Ocean Drilling Program at Site 1308 in the central North Atlantic Ocean. A record of ice-rafted debris was created using census data of the sand fraction from these samples, and a published oxygen isotope stratigraphy for Site 1308 was used to convert core depth to sample age. Abundances of the total terrigenous and total biogenic fraction were plotted against time, as were the abundances of individual grain types in the terrigenous fraction of each sample; these time-series have been examined and interpreted relative to global glacial/interglacial conditions as defined

by Marine Isotope Stages. Provenance of the IRD was also determined using certain terrigenous grain types that have been linked to specific source areas by previous studies.

Goals and Objectives

The overall goal of this research was to determine the abundance record of ice-rafted debris downcore at IODP Site 1308, as well as determine the lithologies of the individual grains in the terrigenous fraction in order to establish the provenance of the IRD. To be more specific, the following research was conducted to:

1. Determine the overall abundance of ice-rafted debris downcore, convert the sample depth within the core to sample age, and produce a record of ice-rafted debris abundance through time. The ice-rafted debris abundance record was then compared to the record of global glacial and interglacial stages to determine the regional response of the circum-North Atlantic to global climate changes; and
2. Identify the lithologies of the grains in the terrigenous fraction of the IRD in order to determine changes in abundance of individual grain types through time. These data were used to establish provenance, or location of origin, of certain grain types based on the known geology of Canada, Greenland, and Iceland. Provenance determinations were then used to identify changes in glacial extent in those source areas through time.

Literature Review

Past studies on ice-rafted debris, such as Krissek & St. John (2002) and St. John & Krissek (2002), have shown that transport by icebergs is the major mechanism for the deposition of relatively large terrigenous grains in mid to high latitude marine settings away from continental margins (Krissek & St. John 2002). In addition, the longest and most complete records of continental glaciations are often determined from studying these sediment sequences due to the greater likelihood of their preservation (St. John & Krissek 2002). In the North Atlantic, the result of these considerations is to choose geographic locations for IRD study based on boundaries described by Ruddiman (1977), away from areas with a high risk for re-erosion such as shelves, canyons, abyssal plains, channels, and fans. These boundaries define an area with sufficient IRD abundance and stratigraphic control to produce a relatively continuous and interpretable record, while emphasizing areas where the sequence is unlikely to be disturbed (Ruddiman 1977). The sampling for this research was then chosen for Site 1308 in the central North Atlantic, in accordance with these guidelines.

The distribution of ice-rafted debris at a site can be interpreted as the record of when continental glaciers extended to coastlines and the IRD components can be used to determine the glaciated regions from which the IRD were transported (Krissek & St. John 2002). Multiple provenance studies have been conducted on ice-rafted sediments in the North Atlantic. Peck et. al. (2007) studied Heinrich events at IODP Site 1308; Heinrich events are sediment layers rich in ice-rafted debris and poor in foraminifera, and have been mapped across the North Atlantic (Peck et al. 2007). The Heinrich events are interpreted to have been deposited during massive discharges of glacial ice from the region around Hudson Strait, which contains a dolomitic carbonate deposit. As a result, the Hudson Strait region is interpreted as the source region for

carbonate rock fragments in cores throughout the North Atlantic (Peck et al. 2007). Krissek & St. John (2002) studied ice rafted debris off the coast of southeast Greenland and concluded that the source of the basaltic IRD was east central Greenland. St. John et al. (2004) studied ice rafted debris off southeast Greenland and concluded that volcanic glass found in the IRD originated from Iceland; they also concluded that basaltic IRD could have originated from Iceland as well as Greenland. St. John et al. (2004) also concluded that hematite-stained quartz IRD could have originated from either the Gulf of St. Lawrence or southern Greenland.

These provenance studies are important because they have identified the source areas for terrigenous grain types examined in this research study. In previous studies, comparing the abundances of these grain types has provided information about the relative rates of IRD supply from each source region over time; a similar approach has been used in this study.

Methods

Site 1308, located in the central North Atlantic, was cored during Expedition 303 of the Integrated Ocean Drilling Program. In order to obtain as complete a stratigraphic record as possible, multiple holes were drilled at this site, and complete intervals were linked between holes to produce a composite section; sample positions within this complete section are indicated by a depth of meters composite depth (mcd). Samples for this study were 10 cm volumes, taken as 2 cm increments, approximately every 25-30 cm downcore.

Prior to this study, the samples were processed to separate the medium sand-and-coarser fraction from the finer-grained sediments, and to determine the abundance (weight percent) of the coarser material. This process included the following steps:

1) the sample was oven-dried at 40°C for 24 hours

2) the dried sample was weighed

3) the sample was disaggregated ultrasonically for 10 minutes in distilled water

4) the sample was wet-sieved at 150 μm and 2mm

5) the 150 μm to 2 mm size fraction was oven-dried at 40°C for 24 hours, and weighed

6) the coarse-fraction abundance (as a weight percent of the total samples) was calculated using the initial dry sample weight and the weight of the coarse fraction.

The coarse fraction is the focus of IRD studies because ice-rafting is the most likely process to transport large grains far offshore.

In this study, 87 samples were studied from an interval of 24.8 meters composite length at Site 1308. The 87 samples studied during this research were taken from 30.78 to 55.58 mcd. Five gaps are present in this range due to missing samples. For each sample, a split of the coarse fraction was examined through a binocular microscope. A representative field of view was

chosen and 100 grains were classified based on standard grain types. The grain types recognized were: quartz, hematite-stained quartz, quartzose rock fragments, coarse-grained mafic rock fragments, fine-grained mafic rock fragments, sedimentary rock fragments, carbonate rock fragments, light-colored volcanic glass, dark-colored volcanic glass, biogenic carbonate, biogenic silica, pyrite, and other (mudballs). The mudballs are accumulations of mud and often other sediment grains that failed to disaggregate during the initial processing of the samples. Individual grains that were not clearly one of the grain types were inspected more thoroughly through physical manipulation using a thin metal rod before the counting took place.

As a measure of data reproducibility, a second representative split from each fifth sample was counted, and the data from the two counts were compared. Table 1 and Table 2 show samples that are of the most similar and most different after a second count was taken. Overall, the replicate analyses show relatively similar results indicating good precision for the IRD data.

Distribution of IRD in Select Split Samples

	Sample (mcd)	Terr %	Bio %	Other %
Most Similar	39.64	46	16	38
	39.64*	46	13	41
	44.98	2	67	31
	44.98*	3	70	27
	46.7	0	82	18
	46.7*	0	82	18
Most Different	48.2	12	30	58
	48.2*	16	31	53
	49.48	3	70	27
	49.48*	6	75	19
	50.33	6	75	19
	50.33*	8	77	16

Table 1: Total percentages in split samples that resulted in the most similar or most different results.

*Denotes second count of that sample

Distribution of Grain Percent in Terrigenous Fraction of Select Split Samples

	Sample (mcd)	%Quartz	%Fe-Quartz	%Quartzose	%Mafic	%Volc	%Sed Frag	%Carb Frag
Most Similar	39.64	60.9	10.9	8.7	2.2	4.3	13.0	0.0
	39.64*	56.5	10.9	8.7	0.0	0.0	23.9	0.0
	44.98	100.0	0.0	0.0	0.0	0.0	0.0	0.0
	44.98*	100.0	0.0	0.0	0.0	0.0	0.0	0.0
	46.7	0.0	0.0	0.0	0.0	0.0	0.0	0.0
	46.7*	0.0	0.0	0.0	0.0	0.0	0.0	0.0
Most Different	48.2	25.0	0.0	16.7	16.7	25.0	16.7	0.0
	48.2*	12.5	0.0	12.5	18.8	37.5	6.2	12.5
	49.48	0.0	0.0	33.3	0.0	33.3	0.0	33.3
	49.48*	0.0	16.7	50.0	0.0	33.3	0.0	0.0
	50.33	16.7	16.7	33.3	16.7	16.7	0.0	0.0
	50.33*	37.5	37.5	12.5	0.0	0.0	12.5	0.0

Table 2: Percentages of individual grain types within the terrigenous fraction of split samples that resulted in the most similar or most different results. Fe-Quartz = Hematite-stained Quartz

*Denotes second count of that sample

After the census of each sample was taken the data were entered into a spreadsheet. Total percentages of terrigenous, biogenic, and other grains out of the 100 total were calculated and each was plotted versus the sample depth (mcd). The terrigenous grains included the quartz, hematite-stained quartz, quartzose rock fragments, coarse-grained mafic rock fragments, fine-grained mafic rock fragments, sedimentary rock fragments, carbonate rock fragments, light-colored volcanic glass, and dark-colored volcanic glass. The biogenic grains included the biogenic carbonate and the biogenic silica. The "other" grains included the pyrite and mudballs.

A published age-depth model for Site 1308 (*Hodell et al.*, 2008) was used to convert sample depth to age and the equivalent graphs were plotted versus time. Because the grains classified as "other" are an undesired dilutant, the abundances of biogenic and terrigenous grains

in each sample were recalculated on an "other-free basis," and were plotted versus time. Lastly, the relative abundance of each terrigenous grain type within the terrigenous fraction only was calculated for each sample, and was plotted versus time. For these calculations, the coarse-grained mafic rock fragments and fine-grained mafic rock fragments were grouped under "mafic rock fragments" and the light-colored volcanic glass and dark-colored volcanic glass were grouped under "volcanic glass," and the different grain types were plotted versus age.

The chronology of marine isotope stages established by Aitken & Stokes (1997) was used to compare this IRD record to globally defined glacial/interglacial stages. According to IRD research conducted by Peck et al. (2007), Krissek & St. John (2002), and St. John et al. (2004), hematite-stained quartz grains, carbonate rock fragments, mafic rock fragments, and volcanic glass are distinctive indications of IRD source areas. The abundances of these grain types within the terrigenous fraction can be used to determine changes in IRD supply through time from Canada-South Greenland and east central Greenland-Iceland, and to place those variations in supply into the context of global glacial/interglacial cycles.

Results

Five samples are missing within the interval studied, leaving gaps in the data and figures. These gaps occur at 41.36, 42.86, 44.72, 45.48, and 47.48 mcd, which correspond to ages of 637, 660, 688, 700, and 730 ka, respectively.

Table 3 is a summary of ice-rafted debris abundances relative to the marine isotope stages defined by Aitken & Stokes (1997). The even-numbered stages represent glacial periods and the odd-numbered stages represent interglacial periods. The youngest age for Stage 13 and oldest age for Stage 21 are limited to ages of the IRD record produced in this study and do not represent the actual stage boundaries determined by Aitken & Stokes (1997). For each marine isotope stage, Table 3 includes the average of the total terrigenous abundances, the average terrigenous abundance when the "other" grains are excluded, the maximum terrigenous abundance for that stage when "other" grains are excluded, and the average abundance of quartz in the terrigenous fraction. The table shows relatively similar abundances of terrigenous grains through each glacial/interglacial stage but distinct differences in maximum percentages between the stages. Multiple interglacial stages have maximum terrigenous abundances that are as large as or larger than the terrigenous abundances during glacial stages, and most notably in Stages 15, 17, and 19. The average quartz abundances in the terrigenous fraction are also relatively similar for each stage, with most falling between 20% and 35%.

Summary of IRD Abundances during Marine Isotope Stages

MIS	Time Interval	Average %Terr	Average %Terr OF	Max %Terr OF	Average %Quartz in Terr
13	525 ka - 528 ka	7	10.1	11.7	69.7
14	528 ka - 568 ka	4.4	6.8	40.0	34.7
15	568 ka - 621 ka	12.9	18.3	82.1	33.0
16	621 ka - 659 ka	10.3	16.9	27.0	44.2
17	659 ka -712 ka	10.2	13.8	97.9	22.4
18	712 ka -760 ka	10.4	22.1	86.4	25.2
19	760 ka - 787 ka	9.8	16.2	94.7	9.0
20	787 ka - 810 ka	5.2	8.1	15.4	23.3
21	810 ka - 853 ka	9.6	14.3	56.9	25.0

Table 3: A summary of the IRD abundances relative to the Marine Isotope Stages; Terr = percent terrigenous grains, Terr OF = terrigenous grains other-free; initial time in MIS-13 and final time of MIS-21 are taken from start and end of IRD record and are not representative of the actual stage intervals; MIS adapted from Aitken & Stokes (1997)

Figures 1-3 show total component abundances versus depth at Site 1308. Figure 1 shows the abundance of terrigenous grains out of the 100 grains counted in each sample, Figure 2 shows the abundance of biogenic grains, and Figure 3 shows the abundance of "other" grains, which are neither terrigenous nor biogenic. The terrigenous grains include quartz, hematite-stained quartz, quartzose rock fragments, coarse-grained mafic rock fragments, fine-grained mafic rock fragments, sedimentary rock fragments, carbonate rock fragments, light-colored volcanic glass, and dark-colored volcanic glass. The biogenic grains include biogenic carbonate, which consists of multiple species of foraminifera, and biogenic silica, which consists of

multiple species of diatoms and radiolarians. The "other" in this research referred to pyrite grains and mud accumulations (mudballs). Overall, biogenic grains are the majority of the grains in most of the samples, followed in abundance by the "other" grains, and then the terrigenous grains. Biogenic grains average 62.6% of each sample, with a maximum of 99% and minimum of 2%. The "other" grains average 27.9% of each sample with a maximum of 78% and a minimum of 1%. The terrigenous grains average 9.5% of each sample with a maximum of 93%. Twenty-six of the 87 samples do not include any terrigenous grains. In the 61 samples that contain terrigenous grains, the terrigenous fraction averages nearly 13.5%.

Figures 4 and 5 show the abundances of terrigenous grains and biogenic grains, respectively, when the "other" grains are excluded. Removing the variable dilution effects of the "other" grains gives a clearer view of the relative abundances of terrigenous grains and biogenic grains. These figures show that biogenic grains generally dominate the coarse fraction of these samples, with relatively isolated peaks of increased terrigenous abundances. In these 87 samples, the abundance of terrigenous grains remained below 20% for all but 18 samples. In the 18 samples with terrigenous abundances above 20%, the highest abundance was 97.9%, and these samples averaged 53.3% terrigenous grains.

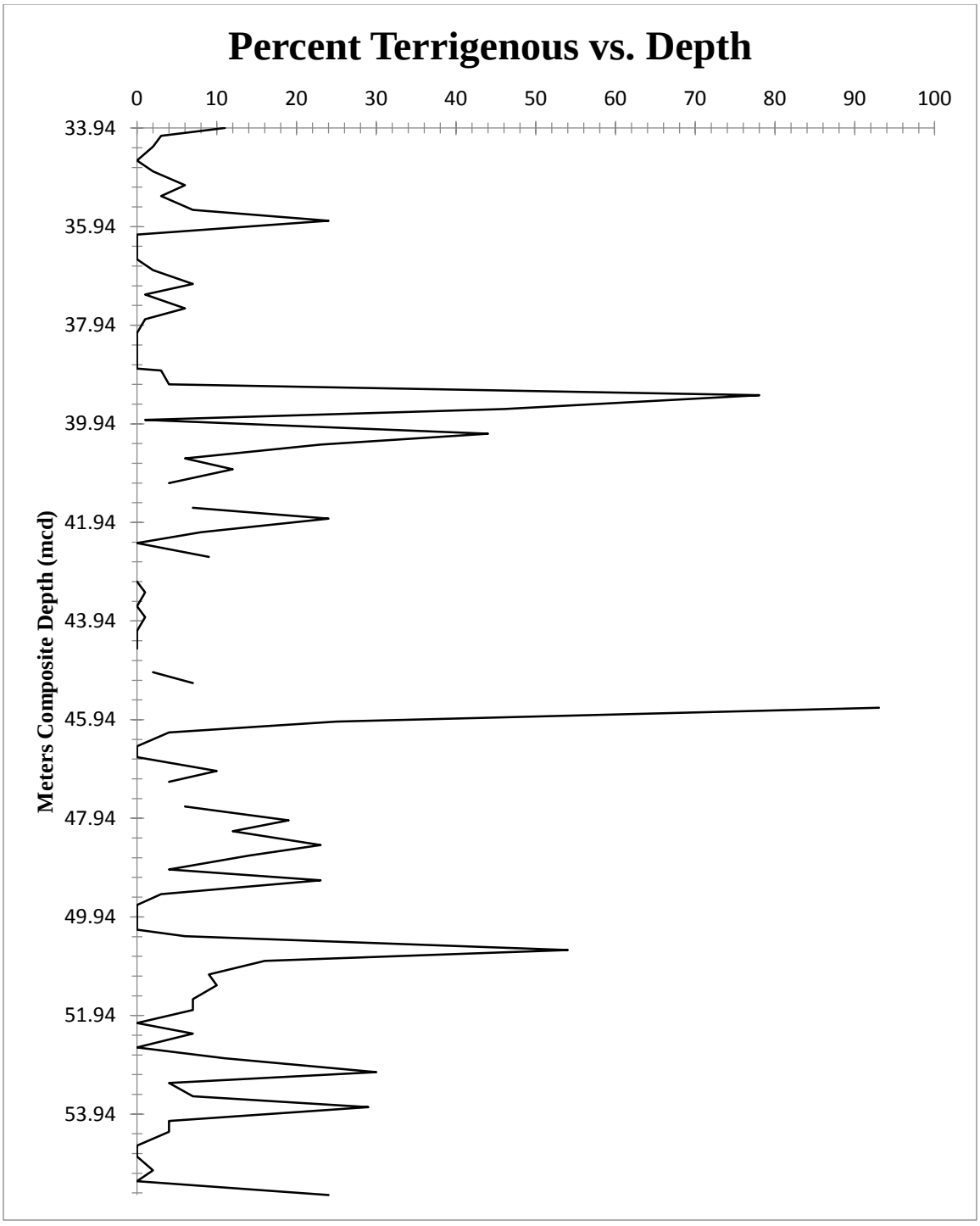

Figure 1: The percent of terrigenous grains out of the 100 counted in each sample versus meters composite depth

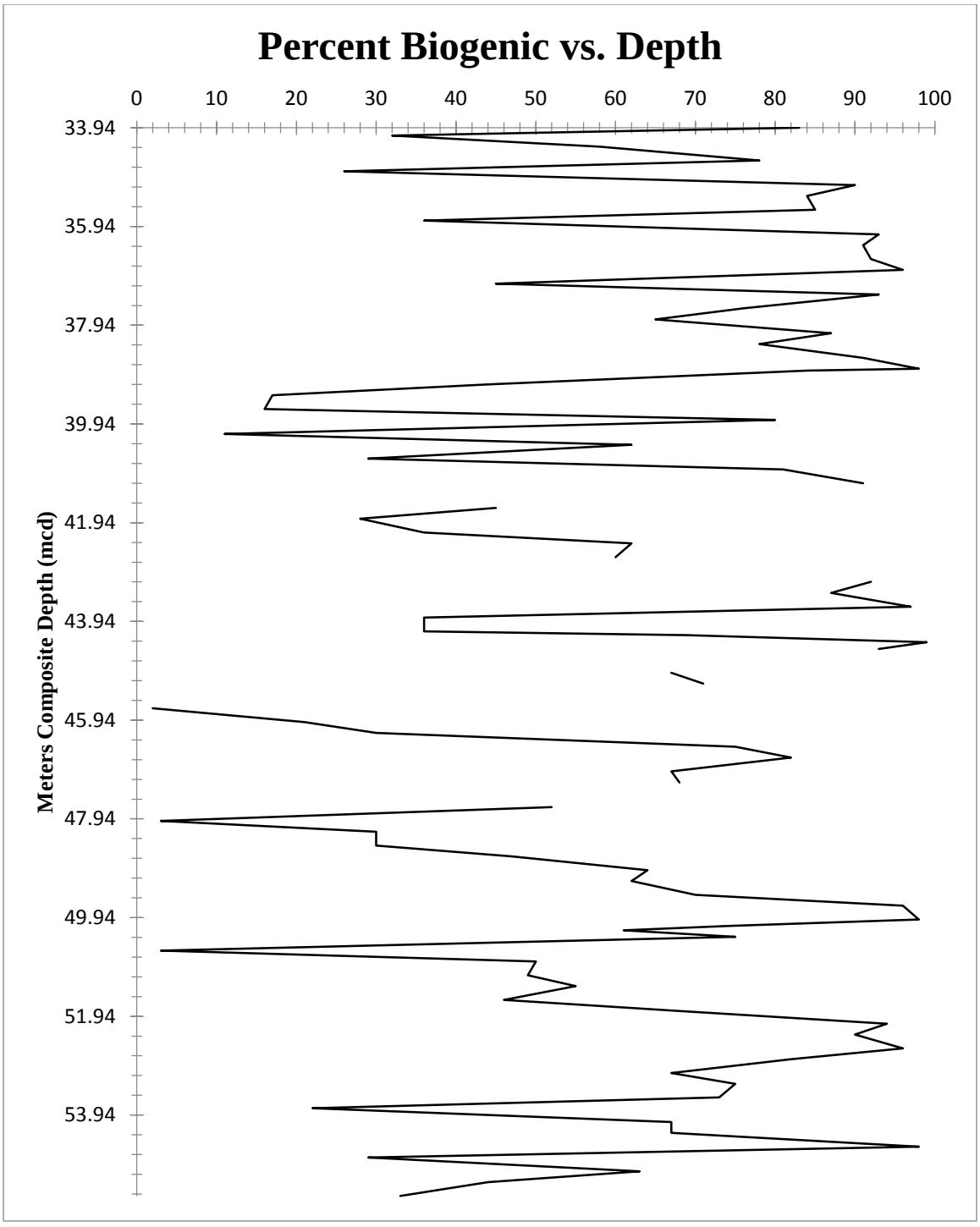

Figure 2: The percent of biogenic grains out of the 100 counted in each sample versus meters composite depth

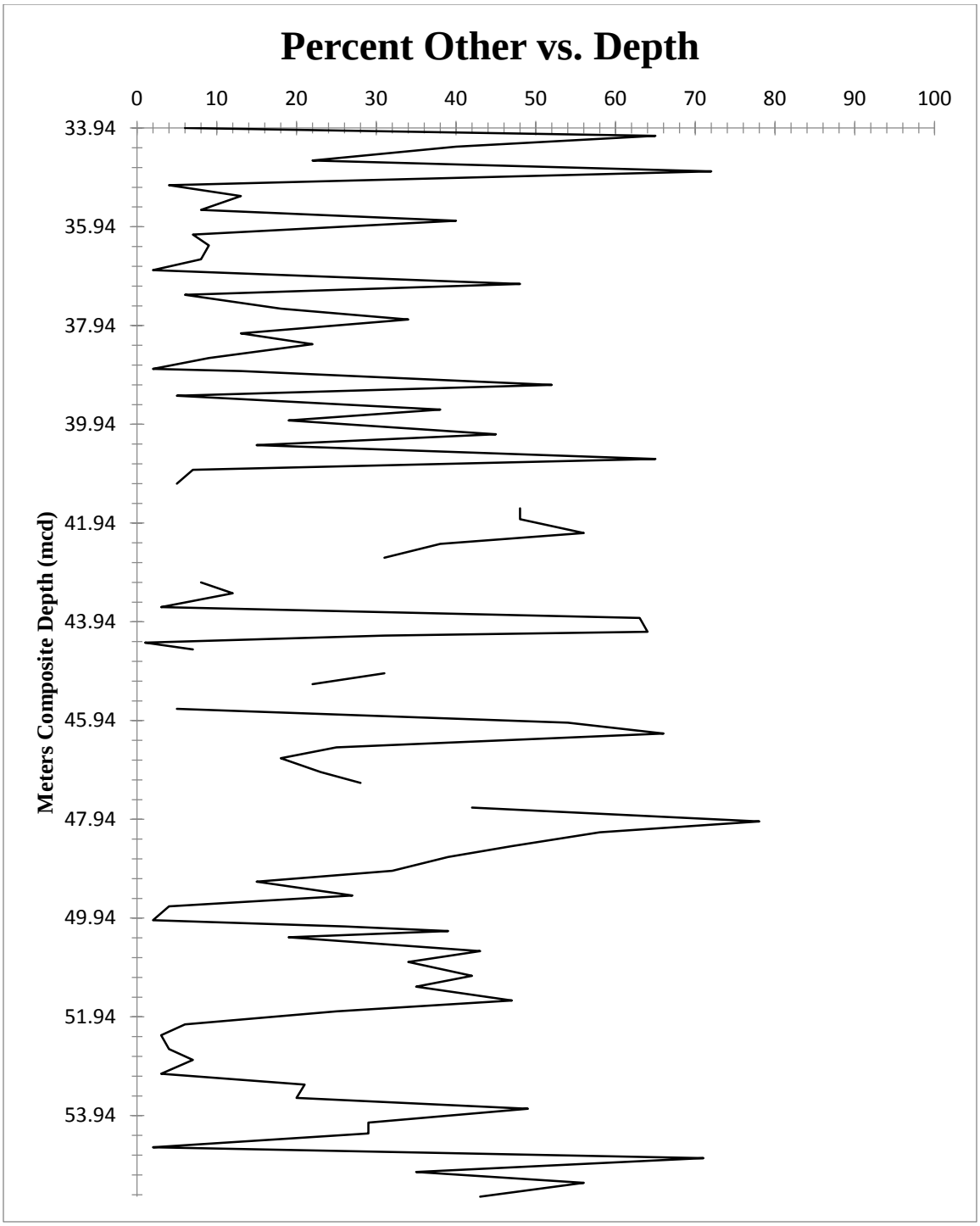

Figure 3: The percent of other grains out of the 100 counted in each sample versus meters composite depth

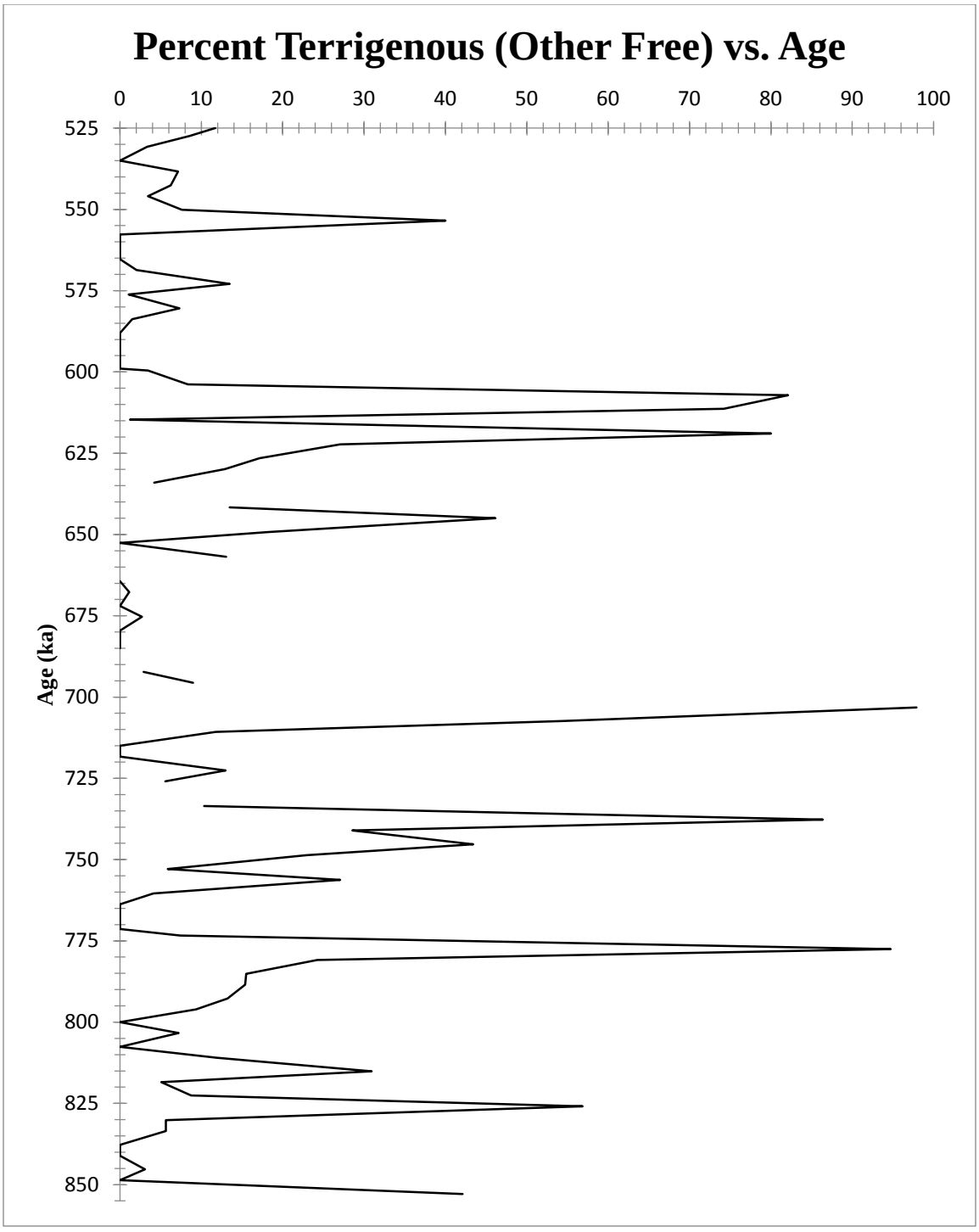

Figure 4: The percent of terrigenous grains in each sample excluding those classified as "other" versus age

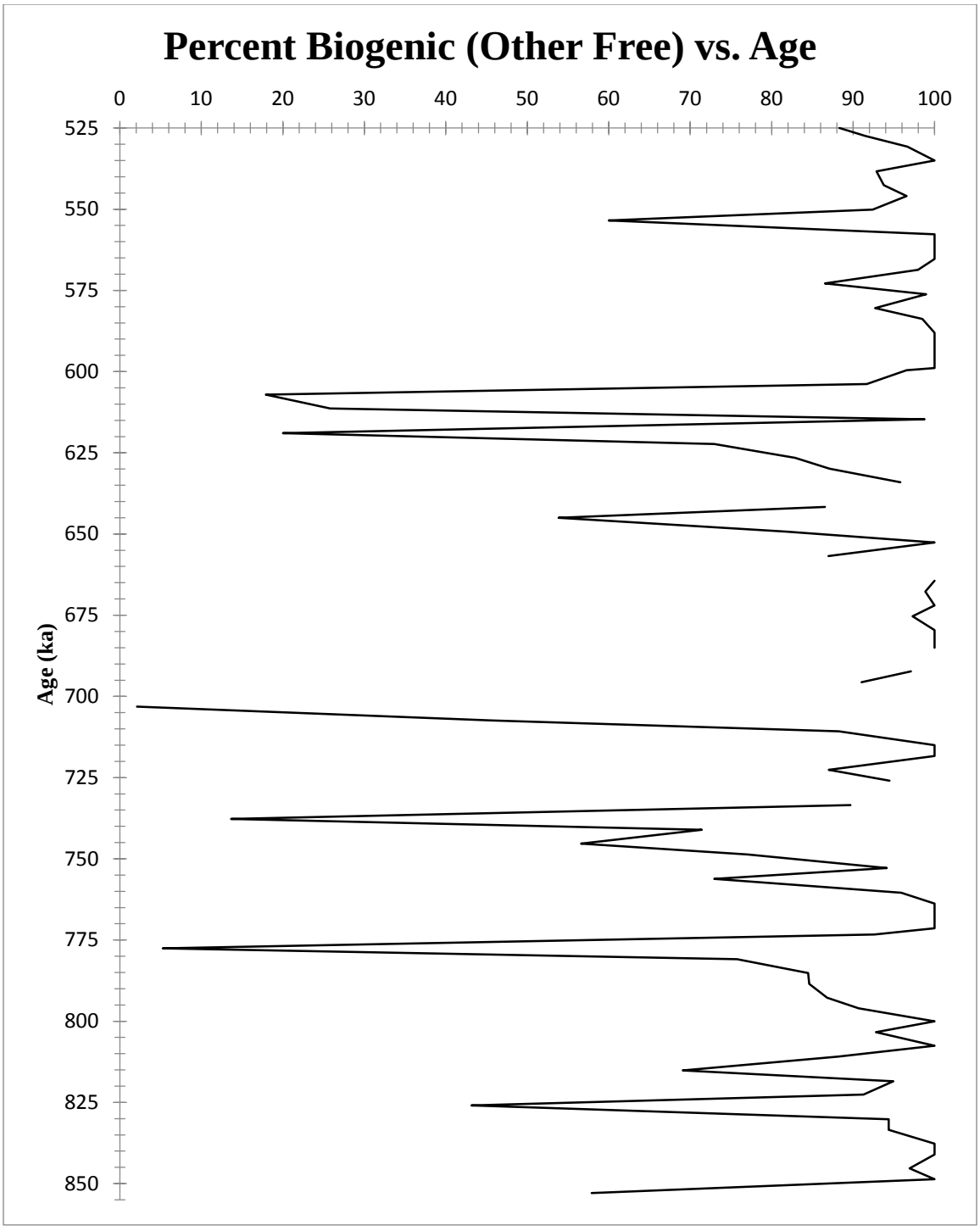

Figure 5: The percent of biogenic grains in each sample excluding those classified as "other" versus age

Figures 6 through 12 show the abundances of individual terrigenous grain types within the terrigenous fraction of each sample; these abundances are plotted as a function of age. The fine-grained mafic rock fragments and coarse-grained mafic rock fragments were combined into "mafic rock fragments" and shown in Figure 9, whereas the light-colored and dark-colored volcanic glass are presented together as "volcanic glass" in Figure 10. Overall, the most abundant grain type is quartz and the least abundant grain type is carbonate rock fragments. In the 61 samples that contain terrigenous grains, the average percentage of quartz in the terrigenous fraction is 40.4% with a maximum of a 100%. The average percentage of hematite-stained quartz is 12.4% with a maximum of 100%. The average percentage of quartzose rock fragments is 12.8% with a maximum of 44.4%. The average percentage of mafic rock fragments is 7.3% with a maximum of 100%. The average percentage of volcanic glass is 12.3% with a maximum of 100%. The average percentage of sedimentary rock fragments is 12.1% with a maximum of 100%. The average percentage of carbonate rock fragments is 2.6% with a maximum of 28.6%. Quartz grains are also the most commonly occurring grain type, being present in 53 of the 61 samples (86.9%). Carbonate rock fragments are the least frequently observed terrigenous grain type being present in 14 of the 61 terrigenous-bearing samples (22.9%).

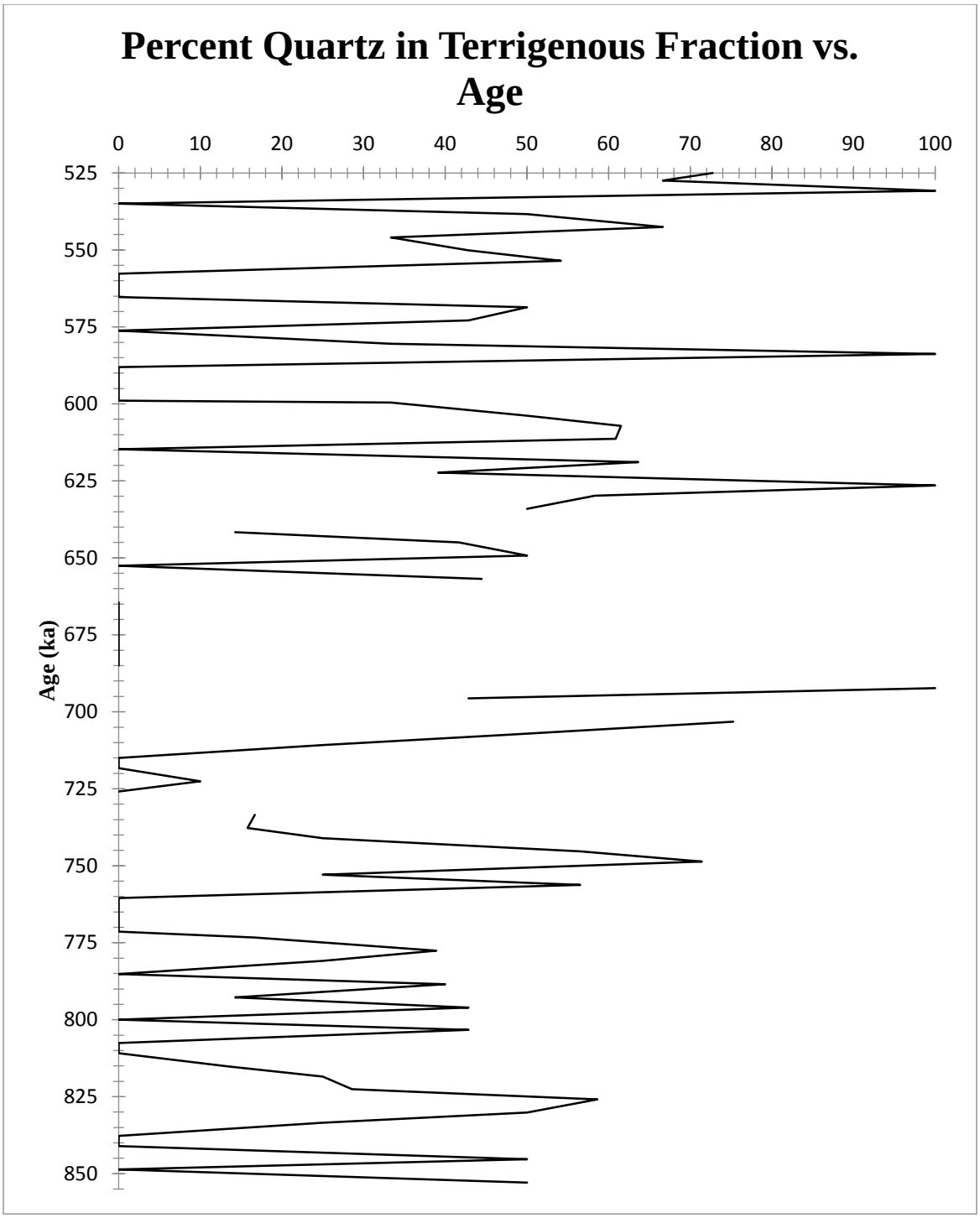

Figure 6: The percentage of quartz grains in the terrigenous fraction of each sample versus age

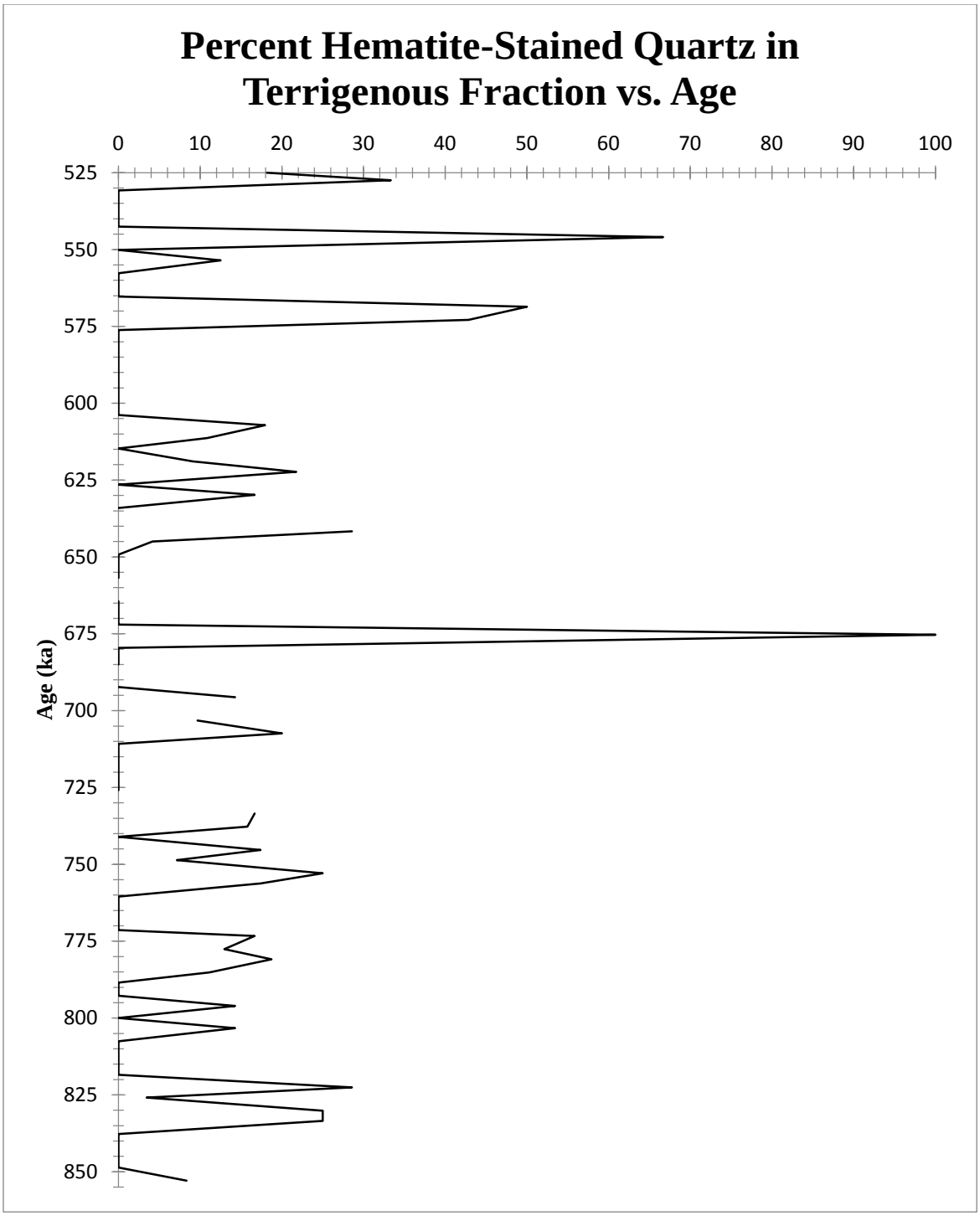

Figure 7: The percentage of hematite-stained quartz grains in the terrigenous fraction of each sample versus age

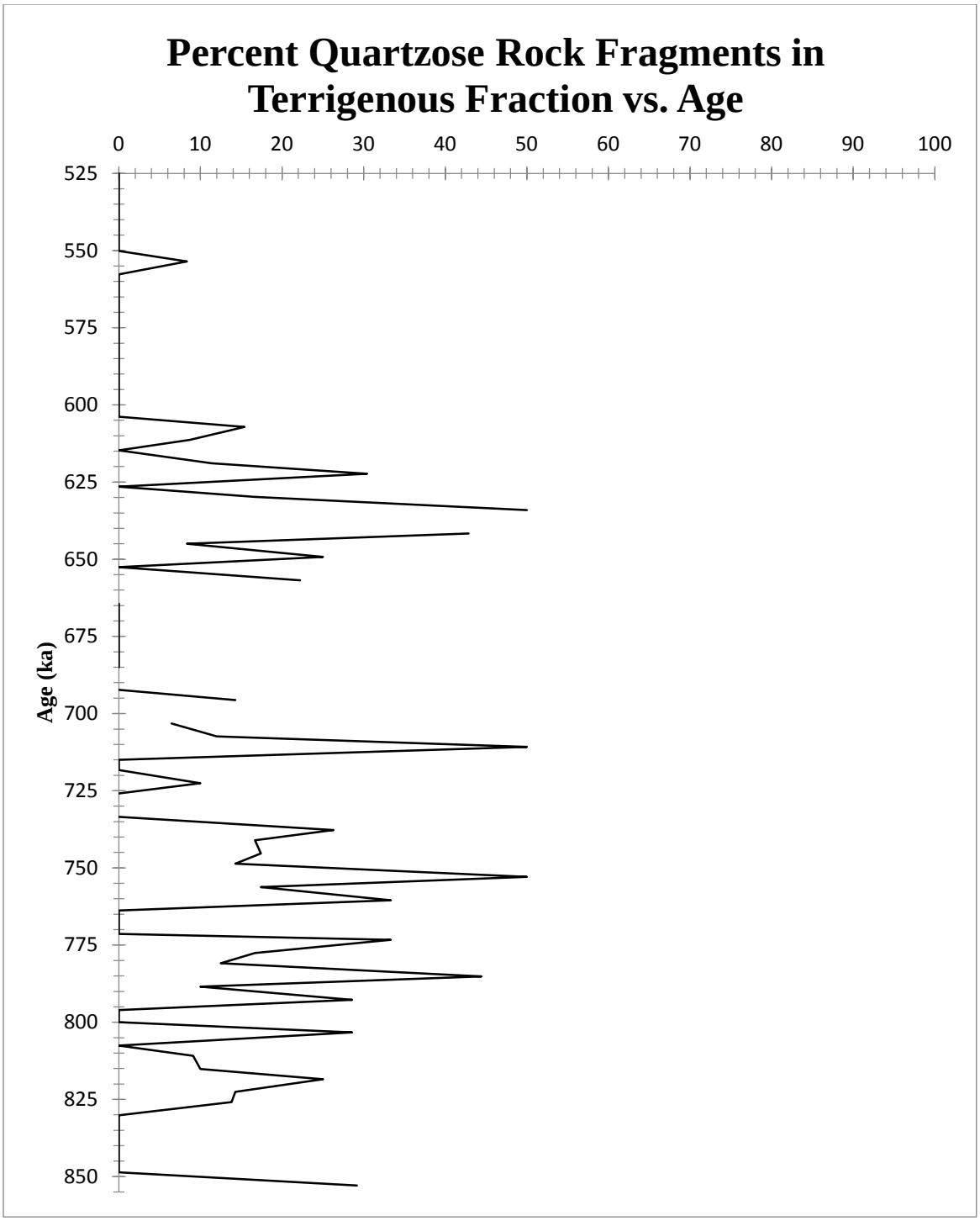

Figure 8: The percentage of quartzose rock fragments in the terrigenous fraction of each sample versus age

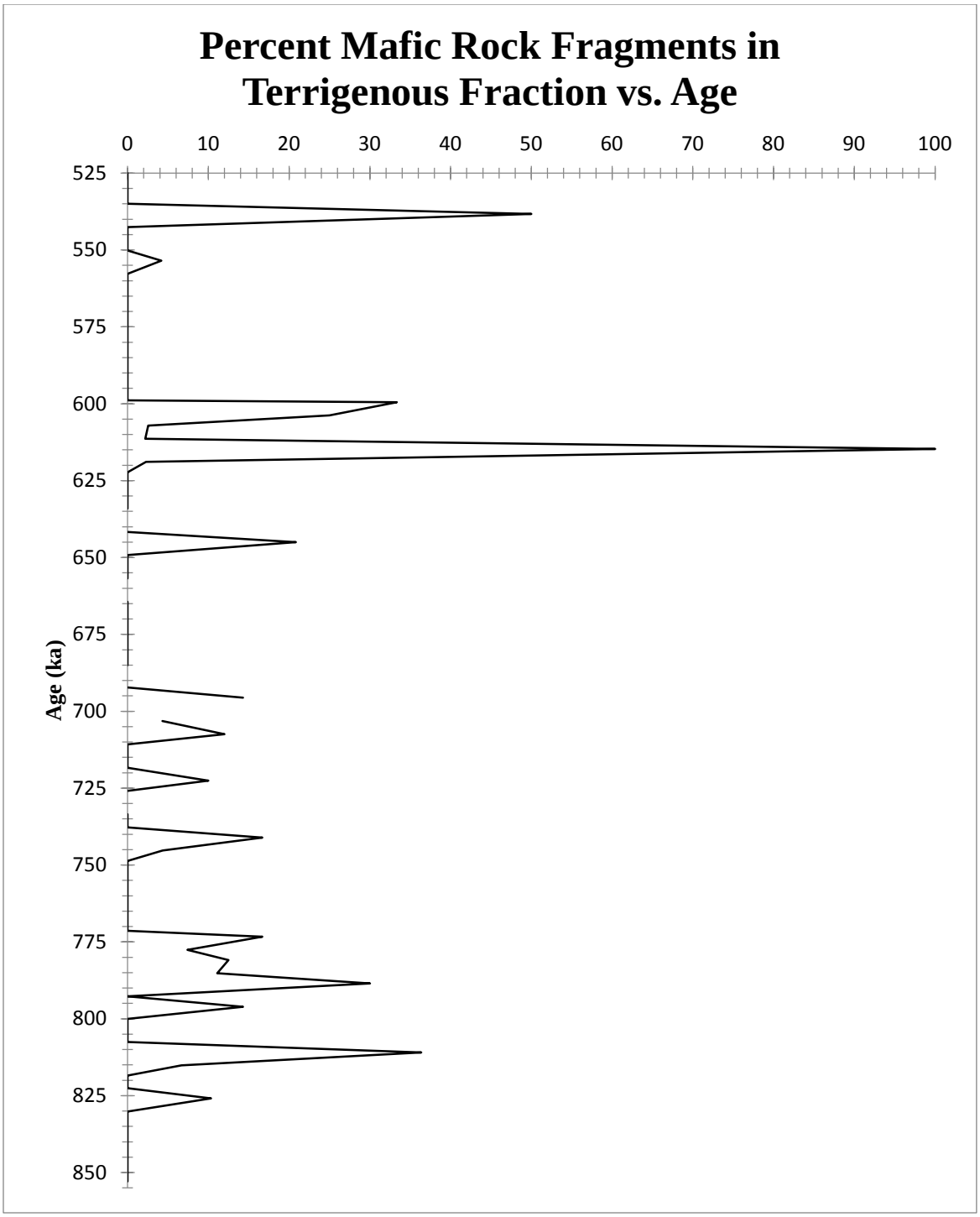

Figure 9: The percentage of mafic rock fragments in the terrigenous fraction of each sample versus age

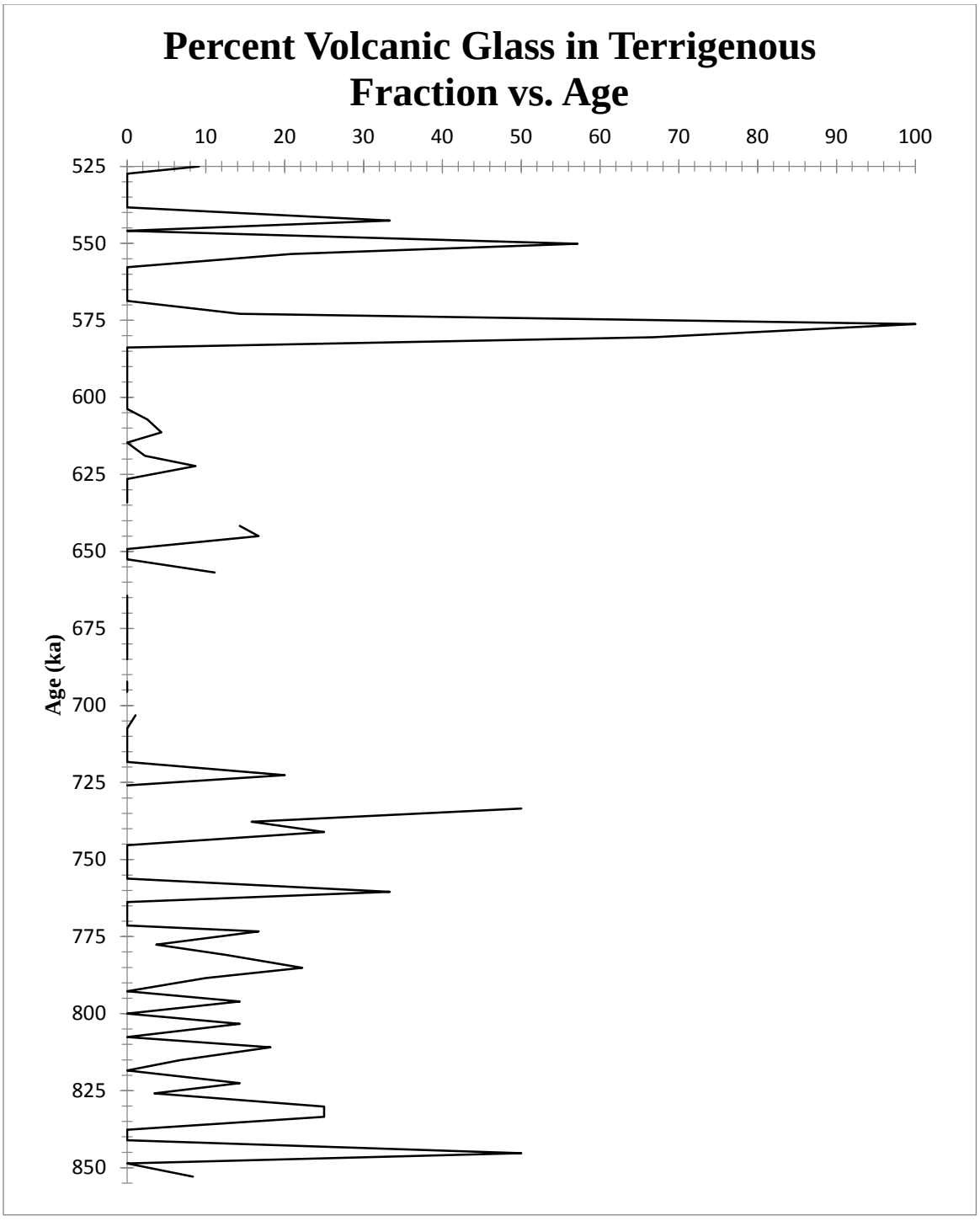

Figure 10: The percentage of volcanic glass fragments in the terrigenous fraction of each sample versus age

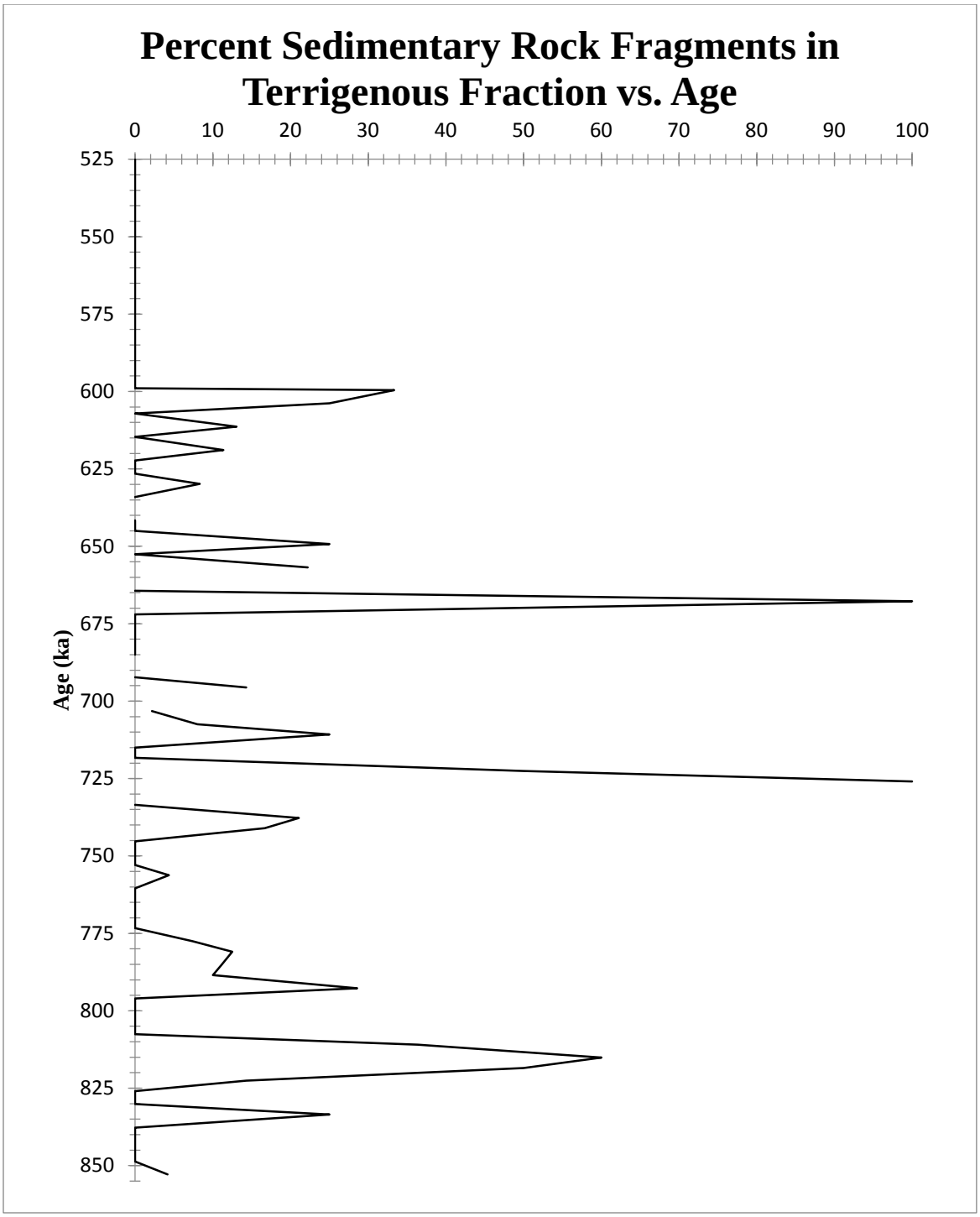

Figure 11: The percentage of sedimentary rock fragments in the terrigenous fraction of each sample versus age excluding carbonate rock fragments

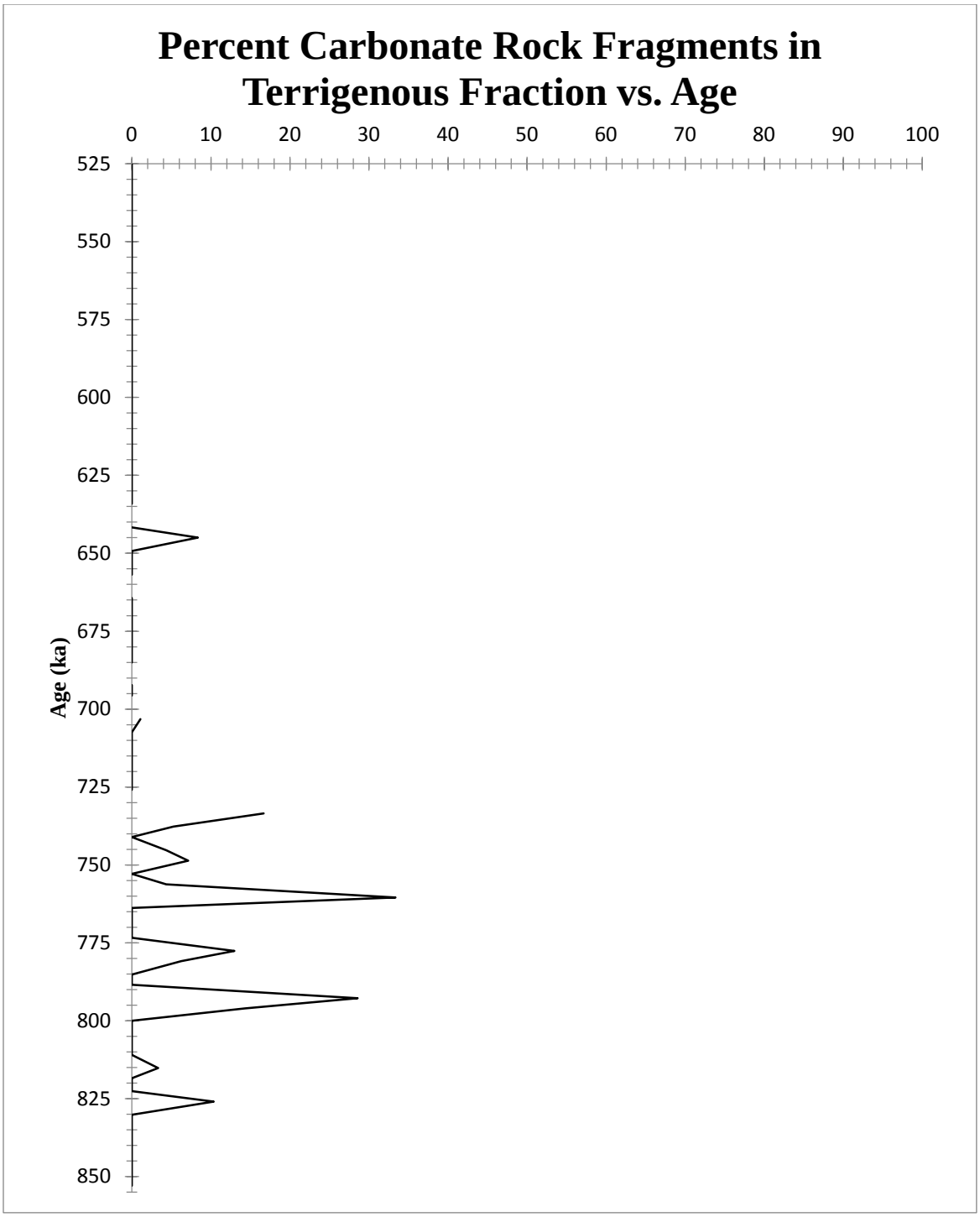

Figure 12: The percentage of carbonate rock fragments in the terrigenous fraction of each sample versus age

Discussion

Fluctuations in IRD Abundance

The results of this study show a record of fluctuating ice-rafted debris abundances over a period of nearly 330 ky with well-defined IRD peaks that do not always occur during the glacial stages defined by Aitken & Stokes (2007). The summary presented in Table 3 suggests a relatively consistent average percentage of ice-rafted debris through both the glacial and the interglacial stages. This is supported by Figure 1 which shows relatively small fluctuations in terrigenous abundance through most of the core with only four relatively large peaks. Removing dilution effects of the "other" grains, as was done for Figure 4, produces a record with larger and more frequent changes in the terrigenous abundance.

Figure 13 is a copy of Figure 4 with the marine isotope stages displayed, and clearly illustrates that peaks in terrigenous abundance occur during both glacial and interglacial periods. The compositions of the 18 high-terrigenous samples that compose these peaks (samples with more than 20% terrigenous grains in the "other-free" distribution) are summarized in Table 4, which highlights the presence of the high terrigenous abundances during interglacial periods. In fact, four of the highest IRD abundances in this record occur during interglacials (Stages 15, 17, and 19), with the terrigenous fraction abundance greater than 80%.

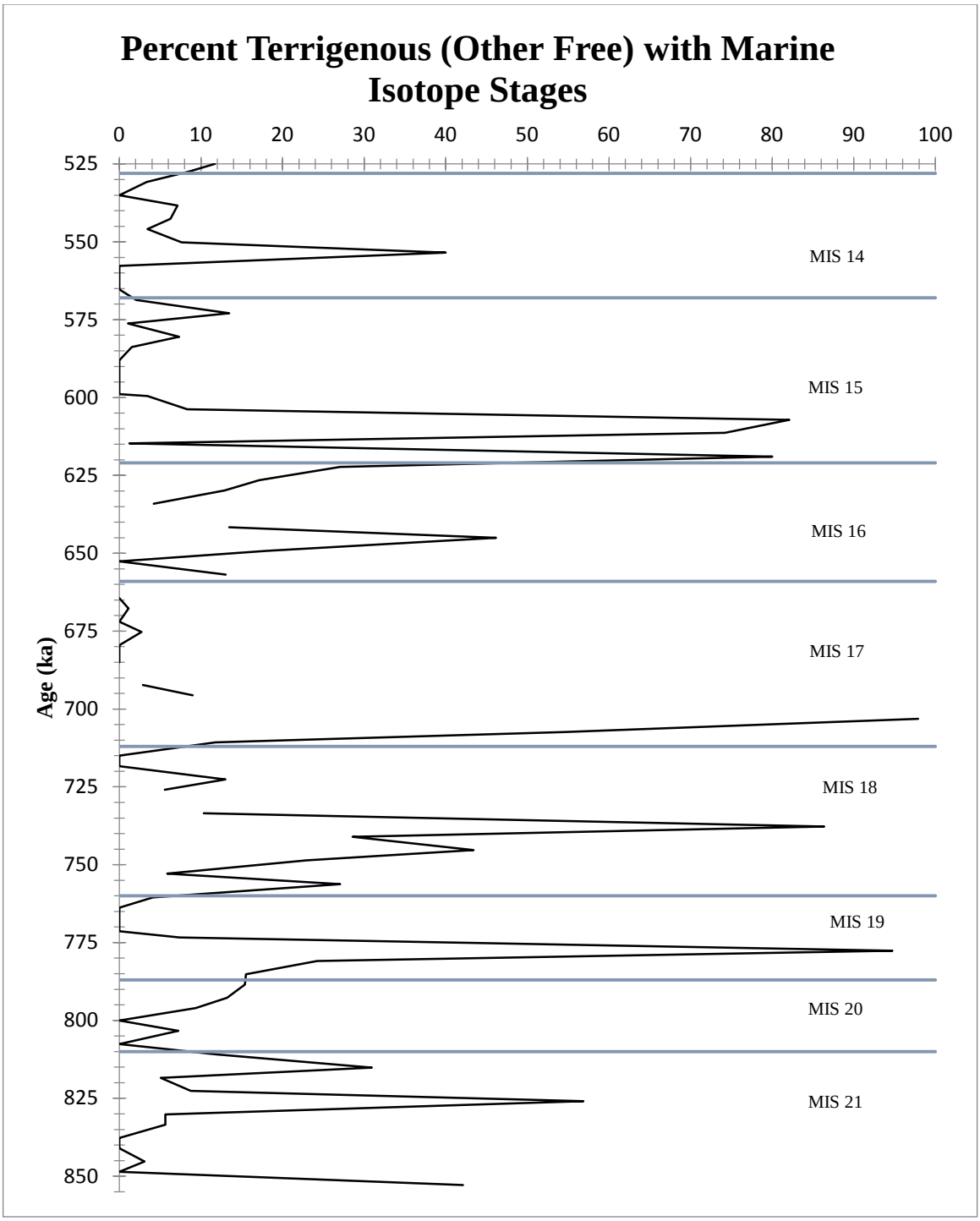

Figure 13: The percentage of terrigenous grains when excluding those classified as "other" with Marine Isotope Stage divisions; applied from Aitken & Stokes (1997)

Distribution of Grain Percent in Terrigenous Fraction in High-Terrigenous Samples (Other Free)

Age (ka)	MIS	Terr Grains	%Terr OF		%Quartz	%Fe-Quartz	%Quartzose	%Mafic	%Volc	%Sed Frag	%Carb Frag
553.5	14	24	40.0		54.2	12.5	8.3	4.2	20.8	0.0	0.0
607.1	15	78	82.1		61.5	17.9	15.4	2.6	2.6	0.0	0.0
611.4	15	46	74.2		60.9	10.9	8.7	2.2	4.3	13.0	0.0
618.9	15	44	80.0		63.6	9.1	11.4	2.3	2.3	11.4	0.0
622.3	16	23	27.1		39.0	21.7	30.4	0.0	8.7	0.0	0.0
645.0	16	24	46.2		41.7	4.2	8.3	20.8	16.7	0.0	8.3
703.2	17	93	97.9		75.3	9.7	6.5	4.3	1.1	2.2	1.1
707.4	17	25	54.3		48.0	20.0	12.0	12.0	0.0	8.0	0.0
737.7	18	19	86.4		15.8	15.8	26.3	0.0	15.8	21.1	5.3
741.0	18	12	28.6		25.0	0.0	16.7	16.7	25.0	16.7	0.0
745.3	18	23	43.4		56.5	17.4	17.4	4.3	0.0	0.0	4.3
748.6	18	14	23.0		71.4	7.1	14.3	0.0	0.0	0.0	7.1
756.2	18	23	27.1		56.5	17.4	17.4	0.0	0.0	4.3	4.3
777.6	19	54	94.7		38.9	13.0	16.7	7.4	3.7	7.4	13.0
780.9	19	16	24.2		25.0	18.8	12.5	12.5	12.5	12.5	6.3
815.2	21	30	30.9		13.3	0.0	10.0	6.7	6.7	60.0	3.3
825.9	21	29	56.9		58.6	3.4	13.8	10.3	3.4	0.0	10.3
852.9	21	24	42.1		50.0	8.3	29.2	0.0	8.3	4.2	0.0
	AVG =	33.4	53.3		47.5	11.5	15.3	5.9	7.3	8.9	3.5

Table 4: A summary of the 18 high-terrigenous samples with percentages of terrigenous, terrigenous (other free), and grain types in terrigenous fraction in relation to the Marine Isotope Stages from Aitken & Stokes (1997); Fe-quartz = hematite-stained quartz

A closer inspection of the IRD peaks during interglacials shows that approximately half of those 10 peaks occur at or relatively close to the glacial-interglacial boundaries. In a study of regional patterns of Pleistocene IRD in the North Pacific, St. John & Krissek (1999) found large IRD peaks during interglacial periods and at the stage boundaries, and concluded that global ice volume was not a dominant control on IRD abundances in that region. In contrast, St. John and Krissek (1999) suggested that more local variations in glacial extent can be significant influences on IRD supplies.

Terrigenous Components

Overall, the abundance variations of the individual terrigenous grain types exhibit patterns similar to the abundance variations of the total terrigenous fraction. Although most abundance peaks for individual grain types still occur near stage boundaries or in glacial stages, no grain type has an abundance pattern that follows the fluctuations in terrigenous fraction abundance exactly.

Quartz is the most abundant grain type in the terrigenous fraction in terms of both frequency of presence and in average abundance within the terrigenous fraction. Quartz abundance variations (Figure 6) generally correspond to changes in the abundance of the total terrigenous fraction, primarily caused by the importance of the quartz in the total IRD. However, quartz abundance also shows some increases during times of low total IRD (e.g. ~530 ka and ~582 ka), and some IRD peaks contain relatively low quartz abundances (e.g., 738 ka and 815 ka).

The hematite-stained quartz and quartzose rock fragments had relatively similar patterns of abundance variations and are less closely linked to changes in total terrigenous abundance. The hematite-stained quartz abundance is consistently 20% or less, with the exception of 4 relatively high peaks. The highest abundance of hematite-stained quartz, at ~675 ka, occurs in a sample with less than 10% total terrigenous material. The abundance pattern for quartzose rock fragments show frequent fluctuations from 20% or slightly below to 40% or slightly higher, as well as intervals less than 50ky long with no quartzose rock fragments.

The abundance patterns for mafic rock fragments and volcanic glass generally showed a different relationship to fluctuations in the total terrigenous abundance than did the other grain types. As shown in Table 4, mafic rock fragment and volcanic glass abundances generally are

low in samples with high total terrigenous abundance. Stages 15 and 17 contain peaks with over 70% terrigenous grains, but the percentages of mafic rock fragments and volcanic glass in these samples are less than 5% each. The peaks with the highest abundance of mafic rock fragments and volcanic glass (e.g. 645, 741, and 781 ka) have some of the lowest total IRD percentages among the IRD peaks identified. In contrast, the abundances of these grain types tend to be highest when total terrigenous abundance is low. The highest percentage of mafic rock fragments is in a sample with total terrigenous abundance less than 2% and mafic rock fragment abundances greater than 30% occur in samples with total IRD abundances less than 15%. The volcanic rock fragments showed similar results with three instances of percentages of over 50% when the total terrigenous fraction is less than 10%.

The sedimentary rock fragments show rather inconsistent changes relative to the total IRD. During periods of high terrigenous abundance the percentage of sedimentary rock fragments generally increases, but some sedimentary rock fragment abundance increases occurred during times of very low terrigenous abundance. In several instances, sedimentary rock fragments are the only terrigenous grain types in a sample with low total IRD. The carbonate rock fragments showed little in relation to the overall terrigenous abundance and appeared to be more isolated occurrences. The carbonate rock fragment percentages were ultimately too small to draw any meaningful conclusions from them.

Provenance

Previous provenance studies on ice-rafted debris in the North Atlantic Ocean include Peck et. al. (2007), Krissek & St. John (2002), and St. John et al. (2004) and many others, which give probable source locations for the hematite-stained quartz, mafic rock fragments, volcanic

glass, and carbonate rock fragments found in the IRD. The carbonate rock fragments can be traced to a dolomitic carbonate platform near Hudson Strait in Canada, but due to the low abundances of carbonate rock fragments in this IRD record from Site 1308, this grain type will not be used here to identify times of IRD supply from that source area (Peck et al. 2007). According to Krissek & St. John (2002), the basaltic IRD can be traced to Tertiary flood basalts in coastal central east Greenland. The more recent study by St. John et al. (2004) concluded that the volcanic glass originated from Iceland, but that basaltic IRD could come from Iceland as well. According to St. John et al. (2004), the hematite-stained quartz most likely originated from the Gulf of the St. Lawrence River in northeastern Canada, although there are other possibilities such as southern Greenland. Quartz and quartzose rock fragments are two of the most abundant IRD but the widespread presence of quartz in the geology of East Greenland devalues their use as an indication for the source area (Krissek & St. John 2002).

Relative rates of IRD input

Comparison of the relative abundances of hematite-stained quartz, mafic rock fragments, and volcanic glass can provide information on the relative ice extent and IRD supply from Canada-southern Greenland compared to east central Greenland-Iceland. If the ratio of hematite-stained quartz to mafic rock fragments or volcanic glass changes over time, it can be inferred that the input of IRD from one of the provenance regions has increased relative to the other.

The hematite-stained quartz abundances compared to the mafic rock fragment abundance show frequent variations, which would suggest multiple changes in IRD output between the two regions. From the start of the core record (853 ka) to approximately 675 ka, the hematite-stained quartz showed relatively steady periods of IRD supply from Canada-southern Greenland,

whereas through the first ~100 ky of this period the abundance of mafic rock fragments showed a decrease in IRD supply from central east Greenland-Iceland. Both lithologies showed rather steady IRD supply from approximately 750 ka until 675 ka, when a large increase in IRD supply from Canada-southern Greenland occurred along with a drop in supply from east central Greenland-Iceland. IRD from Canada-southern Greenland dropped to a steady supply rate from approximately 650-575 ka, whereas at approximately 615 ka, an increase occurred in the IRD supply from central east Greenland-Iceland. From approximately 575 ka to the end of the core data (525 ka), increases in the supply from both Canada-southern Greenland and central east Greenland-Iceland occurred.

Comparison of the hematite-stained quartz abundances with the volcanic glass abundance shows fluctuations in IRD source area importance as well. During the first 150 ky of core data (approximately 850-700 ka), as the IRD supply from Canada-southern Greenland remained relatively steady, the supply from Iceland decreased and then increased again at approximately 740 ka. The increase in IRD supply from Canada-southern Greenland that occurred approximately 675 ka occurred during a period of decreased IRD supply from Iceland that lasted nearly 100 ky (approximately 700-600 ka). Similar to the comparison with the mafic rock fragments, the grain abundances showed increased supply of IRD from both Canada-southern Greenland and central east Greenland-Iceland during the last 50 ky of core (approximately 575-525 ka).

The compositional changes observed when comparing the hematite-stained quartz, mafic rock fragments, and volcanic glass indicate that IRD supply rates from different sources did not change synchronously. This suggests that the fluctuations in supply from each source were not

due to global glacial/interglacial conditions, but more likely in response to local glaciologic controls.

Conclusions

Visual grain counts of the medium-to-very coarse sand fraction have been used to produce an ice-rafted debris record spanning 525-853 ka and 24.8 meters composite of core at IODP Site 1308. Eighty-seven sediment samples were studied under a binocular microscope and 100 grains were counted in each sample by grain type. The abundances of terrigenous, biogenic, and "other" grains in each sample were calculated, as well as the abundances of terrigenous and biogenic fractions without the "other" component. The total terrigenous abundances are interpreted as an IRD indicator, and were compared with the globally defined sequence of Marine Isotope Stages. The abundance of the total terrigenous sediment (IRD) increased during glacial stages and near glacial-interglacial boundaries, a conclusion that has been supported by other IRD studies.

The abundances of individual terrigenous grain types were calculated and compared to the total abundances of the terrigenous fraction. Abundances of individual grain types generally followed the same pattern as the abundances of the total terrigenous fraction, with increases during glacial stages and at or near glacial-interglacial boundaries. In detail, however, the abundance variations of the individual terrigenous components did not directly follow changes in the total terrigenous abundance; instead, changes in component abundances differed in the details of timing and the relative amounts of change. Quartz was the most abundant grain type in the terrigenous fraction, and carbonate rock fragments were the least abundant. In multiple cases, mafic rock fragments and volcanic glass became more abundant within the terrigenous fraction

as the abundance of the overall terrigenous fraction decreased, and these two components showed little increase when the total terrigenous abundance was high. This behavior implies that the mafic rock fragments and volcanic glass make up a large percentage of the IRD deposited during times of relatively low IRD input, and continued at a relatively slow input rate during times of rapid IRD supply. Previous provenance studies indicate that the mafic rock fragments originate from east central Greenland or Iceland, and the volcanic glass originates from Iceland. Hematite-stained quartz in the IRD originated from northeastern Canada or southern Greenland, and carbonate rock fragments originated from the area surrounding Hudson Strait. Based on these provenance interpretations and the relative abundances of hematite-stained quartz to mafic rock fragments and volcanic glass, the relative rates of IRD input were determined for the source areas of northeastern Canada-southern Greenland and east central Greenland-Iceland. These comparisons show frequent and sometimes dramatic fluctuations in the ratio of hematite-stained quartz to mafic rock fragments and to volcanic glass, which suggests frequent changes in the major IRD sources through time. These relative abundance changes also indicate the IRD supplies from the various source areas did not change synchronously through the interval studied. This record suggests that the IRD input from Iceland and central East Greenland was relatively slow and consistent through both glacials and interglacials. The larger change was increased supply of quartz, hematite-stained quartz, and quartzose rock fragments from Canada and south Greenland during glacials and at transitions, with significantly lower input from these areas during the interglacials.

Recommendations for future work

The IRD record produced by this study can be improved by reprocessing the samples to remove biogenic carbonate and mudballs. Many of the samples used in this study contained a high percentage of mudballs, frequently near 50% of the total sample. Additional or new disaggregating treatments could potentially decrease the amount of mudballs in the samples, therefore providing a more accurate count of "real" sediment grains. The samples were originally treated with an ultrasonic bath, and additional ultrasonic treatment may successfully disaggregate the remaining mudballs. Alternatively, different disaggregation methods such as gentle hand grinding of the samples with mortar and pestle could also be tested. Comparison of census data from this study to a recounting of the samples after further disaggregation might produce a more accurate IRD record, and also identify potential inaccuracies in previous studies conducted with the methods used here. To get more accurate weight percentages of the terrigenous fraction, an acid bath could also be used to dissolve the biogenic carbonate and leave the terrigenous grains intact.

Extension of the study farther downcore will extend the IRD record and will begin to identify the potential effects of the Mid-Pleistocene Climate Transition (MPCT) on ice-rafting in the North Atlantic. The Mid-Pleistocene Climate Transition is a major feature in many proxy records of paleoclimate between ~600 ka and 1 Ma; because this IRD record does not extend through the entire possible interval of the MPCT, however, it is not possible to identify any signal of the MCPT here.

References Cited

Aitken, Martin J., and Stephen Stokes. 1997. Climatostratigraphy. *Chronometric Dating in Archaeology*. Springer US. 1-30.

Hodell, David A., James E. T. Channell, Jason H. Curtis, Oscar E. Romero, and Ursula Röhl. Onset of "Hudson Strait" Heinrich Events in the Eastern North Atlantic at the End of the Middle Pleistocene Transition (~640 Ka)? Paleoceanography 23.4 (2008).

Krissek, L.A., and St. John, K., 2002. Pleistocene iceberg production from East Greenland: synchronous between source areas, but distinct from global ice volume. Bulletin of the Geological Society of Denmark, 49, 79-89.

Peck, V. L., Hall, I. R., Zahn, R., Grousset, F., Hemming, S. R., and Sourse, J. D., 2007, The relationship of Heinrich events and their European precursors over the past 60 kyr BP: a multi-proxy ice rafted debris provenance study in the North East Atlantic, Quaternary Science Reviews, 26, 862-875.

Ruddiman, William F. Late Quaternary deposition of ice-rafted sand in the subpolar North Atlantic (lat 40 to 65 N). Geological Society of America Bulletin 88.12 (1977): 1813-1827.

St. John, K.E.K., B.P. Flower, and L. Krissek, 2004. Evolution of iceberg melt, biological productivity, and the record of Icelandic volcanism in the Irminger basin since 630 ka. Marine Geology, 212, 133-152.

St. John, K.E.K., and L.A. Krissek, 1999. Regional patterns of Pleistocene IRD flux in the North Pacific. Paleoceanography, 14, 653-662.

St. John, K., and L.A. Krissek, 2002. The late Miocene to Pleistocene ice-rafting history of southeast Greenland. Boreas, 31, 28-35.

Appendix: Grain Distributions Downcore

Depth (mcd)	AGE (ka)	%Terr	%Bio	%Other	%Quartz	%Fe-Quartz	%Quartz-ose	%Mafic	%Volc	%Sed Frag	%Carb Frag
33.94	525.0	11.0	83.0	6.0	72.7	18.2	0.0	0.0	9.1	0.0	0.0
34.1	527.4	3.0	32.0	65.0	66.7	33.3	0.0	0.0	0.0	0.0	0.0
34.32	530.8	2.0	58.0	40.0	100.0	0.0	0.0	0.0	0.0	0.0	0.0
34.6	535.0	0.0	78.0	22.0	0.0	0.0	0.0	0.0	0.0	0.0	0.0
34.82	538.3	2.0	26.0	72.0	50.0	0.0	0.0	50.0	0.0	0.0	0.0
34.82*	538.3	2.0	21.0	77.0	50.0	0.0	0.0	0.0	0.0	50.0	0.0
35.1	542.6	6.0	90.0	4.0	66.7	0.0	0.0	0.0	33.3	0.0	0.0
35.32	545.9	3.0	84.0	13.0	33.3	66.7	0.0	0.0	0.0	0.0	0.0
35.6	550.2	7.0	85.0	8.0	42.9	0.0	0.0	0.0	57.1	0.0	0.0
35.82	553.5	24.0	36.0	40.0	54.2	12.5	8.3	4.2	20.8	0.0	0.0
36.1	557.7	0.0	93.0	7.0	0.0	0.0	0.0	0.0	0.0	0.0	0.0
36.1*	557.7	0.0	95.0	5.0	0.0	0.0	0.0	0.0	0.0	0.0	0.0
36.32	561.1	0.0	91.0	9.0	0.0	0.0	0.0	0.0	0.0	0.0	0.0
36.6	565.3	0.0	92.0	8.0	0.0	0.0	0.0	0.0	0.0	0.0	0.0
36.82	568.6	2.0	96.0	2.0	50.0	50.0	0.0	0.0	0.0	0.0	0.0
37.1	572.9	7.0	45.0	48.0	42.9	42.9	0.0	0.0	14.3	0.0	0.0
37.32	576.2	1.0	93.0	6.0	0.0	0.0	0.0	0.0	100.0	0.0	0.0
37.32*	576.2	0.0	95.0	5.0	0.0	0.0	0.0	0.0	0.0	0.0	0.0
37.6	580.5	6.0	76.0	18.0	33.3	0.0	0.0	0.0	66.7	0.0	0.0
37.82	583.8	1.0	65.0	34.0	100.0	0.0	0.0	0.0	0.0	0.0	0.0
38.1	588.0	0.0	87.0	13.0	0.0	0.0	0.0	0.0	0.0	0.0	0.0
38.32	591.4	0.0	78.0	22.0	0.0	0.0	0.0	0.0	0.0	0.0	0.0
38.6	595.6	0.0	91.0	9.0	0.0	0.0	0.0	0.0	0.0	0.0	0.0
38.6*	595.6	0.0	90.0	10.0	0.0	0.0	0.0	0.0	0.0	0.0	0.0
38.82	598.9	0.0	98.0	2.0	0.0	0.0	0.0	0.0	0.0	0.0	0.0
38.86	599.5	3.0	84.0	13.0	33.3	0.0	0.0	33.3	0.0	33.3	0.0
39.14	603.8	4.0	44.0	52.0	50.0	0.0	0.0	25.0	0.0	25.0	0.0
39.36	607.1	78.0	17.0	5.0	61.5	17.9	15.4	2.6	2.6	0.0	0.0
39.64	611.4	46.0	16.0	38.0	60.9	10.9	8.7	2.2	4.3	13.0	0.0
39.64*	611.4	46.0	13.0	41.0	56.5	10.9	8.7	0.0	0.0	23.9	0.0
39.86	614.7	1.0	80.0	19.0	0.0	0.0	0.0	100.0	0.0	0.0	0.0
40.14	618.9	44.0	11.0	45.0	63.6	9.1	11.4	2.3	2.3	11.4	0.0
40.36	622.3	23.0	62.0	15.0	39.1	21.7	30.4	0.0	8.7	0.0	0.0

Total terrigenous, biogenic, and "other" abundances downcore; individual grain abundances within terrigenous fraction

*Denotes second count of sample (for the twice-split samples)

[x] Denotes missing sample

Depth (mcd)	AGE (ka)	%Terr	%Bio	%Other	%Quartz	%Fe-Quartz	%Quartz-ose	%Mafic	%Volc	%Sed Frag	%Carb Frag
40.64	626.5	6.0	29.0	65.0	100.0	0.0	0.0	0.0	0.0	0.0	0.0
40.86	629.8	12.0	81.0	7.0	58.3	16.7	16.7	0.0	0.0	8.3	0.0
40.86*	629.8	16.0	71.0	13.0	56.3	12.5	18.8	0.0	6.3	6.3	0.0
41.14	634.1	4.0	91.0	5.0	50.0	0.0	50.0	0.0	0.0	0.0	0.0
41.36[x]	637.4										
41.64	641.7	7.0	45.0	48.0	14.3	28.6	42.9	0.0	14.3	0.0	0.0
41.86	645.0	24.0	28.0	48.0	41.7	4.2	8.3	20.8	16.7	0.0	8.3
42.14	649.2	8.0	36.0	56.0	50.0	0.0	25.0	0.0	0.0	25.0	0.0
42.36	652.6	0.0	62.0	38.0	0.0	0.0	0.0	0.0	0.0	0.0	0.0
42.36*	652.6	0.0	68.0	32.0	0.0	0.0	0.0	0.0	0.0	0.0	0.0
42.64	656.8	9.0	60.0	31.0	44.4	0.0	22.2	0.0	11.1	22.2	0.0
42.86[x]	660.2										
43.14	664.4	0.0	92.0	8.0	0.0	0.0	0.0	0.0	0.0	0.0	0.0
43.36	667.7	1.0	87.0	12.0	0.0	0.0	0.0	0.0	0.0	100.0	0.0
43.64	672.0	0.0	97.0	3.0	0.0	0.0	0.0	0.0	0.0	0.0	0.0
43.86	675.3	1.0	36.0	63.0	0.0	100.0	0.0	0.0	0.0	0.0	0.0
43.86*	675.3	0.0	27.0	73.0	0.0	0.0	0.0	0.0	0.0	0.0	0.0
44.14	679.5	0.0	36.0	64.0	0.0	0.0	0.0	0.0	0.0	0.0	0.0
44.22	680.8	0.0	69.0	31.0	0.0	0.0	0.0	0.0	0.0	0.0	0.0
44.36	682.9	0.0	99.0	1.0	0.0	0.0	0.0	0.0	0.0	0.0	0.0
44.5	685.0	0.0	93.0	7.0	0.0	0.0	0.0	0.0	0.0	0.0	0.0
44.72[x]	688.3										
44.98	692.3	2.0	67.0	31.0	100.0	0.0	0.0	0.0	0.0	0.0	0.0
44.98*	692.3	3.0	70.0	27.0	100.0	0.0	0.0	0.0	0.0	0.0	0.0
45.2	695.6	7.0	71.0	22.0	42.9	14.3	14.3	14.3	0.0	14.3	0.0
45.48[x]	699.8										
45.7	703.2	93.0	2.0	5.0	75.3	9.7	6.5	4.3	1.1	2.2	1.1
45.98	707.4	25.0	21.0	54.0	48.0	20.0	12.0	12.0	0.0	8.0	0.0
46.2	710.8	4.0	30.0	66.0	25.0	0.0	50.0	0.0	0.0	25.0	0.0
46.48	715.0	0.0	75.0	25.0	0.0	0.0	0.0	0.0	0.0	0.0	0.0
46.7	718.3	0.0	82.0	18.0	0.0	0.0	0.0	0.0	0.0	0.0	0.0
46.7*	718.3	0.0	82.0	18.0	0.0	0.0	0.0	0.0	0.0	0.0	0.0
46.98	722.6	10.0	67.0	23.0	10.0	0.0	10.0	10.0	20.0	50.0	0.0

Total terrigenous, biogenic, and "other" abundances downcore; individual grain abundances within terrigenous fraction

*Denotes second count of sample (for the twice-split samples)

[x] Denotes missing sample

Depth (mcd)	AGE (ka)	%Terr	%Bio	%Other	%Quartz	%Fe-Quartz	%Quartz-ose	%Mafic	%Volc	%Sed Frag	%Carb Frag
47.2	725.9	4.0	68.0	28.0	0.0	0.0	0.0	0.0	0.0	100.0	0.0
47.48[x]	730.2										
47.7	733.5	6.0	52.0	42.0	16.7	16.7	0.0	0.0	50.0	0.0	16.7
47.98	737.7	19.0	3.0	78.0	15.8	15.8	26.3	0.0	15.8	21.1	5.3
48.2	741.1	12.0	30.0	58.0	25.0	0.0	16.7	16.7	25.0	16.7	0.0
48.2*	741.1	16.0	31.0	53.0	12.5	0.0	12.5	18.8	37.5	6.3	12.5
48.48	745.3	23.0	30.0	47.0	56.5	17.4	17.4	4.3	0.0	0.0	4.3
48.7	748.6	14.0	47.0	39.0	71.4	7.1	14.3	0.0	0.0	0.0	7.1
48.98	752.9	4.0	64.0	32.0	25.0	25.0	50.0	0.0	0.0	0.0	0.0
49.2	756.2	23.0	62.0	15.0	56.5	17.4	17.4	0.0	0.0	4.3	4.3
49.48	760.5	3.0	70.0	27.0	0.0	0.0	33.3	0.0	33.3	0.0	33.3
49.48*	760.5	6.0	75.0	19.0	0.0	16.7	50.0	0.0	33.3	0.0	0.0
49.7	763.8	0.0	96.0	4.0	0.0	0.0	0.0	0.0	0.0	0.0	0.0
49.98	768.0	0.0	98.0	2.0	0.0	0.0	0.0	0.0	0.0	0.0	0.0
50.11	770.0	0.0	74.0	26.0	0.0	0.0	0.0	0.0	0.0	0.0	0.0
50.2	771.4	0.0	61.0	39.0	0.0	0.0	0.0	0.0	0.0	0.0	0.0
50.33	773.3	6.0	75.0	19.0	16.7	16.7	33.3	16.7	16.7	0.0	0.0
50.33*	773.3	8.0	77.0	16.0	37.5	37.5	12.5	0.0	0.0	12.5	0.0
50.61	777.6	54.0	3.0	43.0	38.9	13.0	16.7	7.4	3.7	7.4	13.0
50.83	780.9	16.0	50.0	34.0	25.0	18.8	12.5	12.5	12.5	12.5	6.3
51.11	785.2	9.0	49.0	42.0	0.0	11.1	44.4	11.1	22.2	11.1	0.0
51.33	788.5	10.0	55.0	35.0	40.0	0.0	10.0	30.0	10.0	10.0	0.0
51.61	792.7	7.0	46.0	47.0	14.3	0.0	28.6	0.0	0.0	28.6	28.6
51.61*	792.7	8.0	49.0	43.0	25.0	12.5	12.5	0.0	12.5	37.5	0.0
51.83	796.1	7.0	68.0	25.0	42.9	14.3	0.0	14.3	14.3	0.0	14.3
52.09	800.0	0.0	94.0	6.0	0.0	0.0	0.0	0.0	0.0	0.0	0.0
52.31	803.3	7.0	90.0	3.0	42.9	14.3	28.6	0.0	14.3	0.0	0.0
52.59	807.6	0.0	96.0	4.0	0.0	0.0	0.0	0.0	0.0	0.0	0.0
52.81	810.9	11.0	82.0	7.0	0.0	0.0	9.1	36.4	18.2	36.4	0.0
53.09	815.2	30.0	67.0	3.0	13.3	0.0	10.0	6.7	6.7	60.0	3.3
53.09*	815.2	29.0	68.0	3.0	24.1	3.4	10.3	10.3	6.9	44.8	0.0
53.31	818.5	4.0	75.0	21.0	25.0	0.0	25.0	0.0	0.0	50.0	0.0
53.58	822.6	7.0	73.0	20.0	28.6	28.6	14.3	0.0	14.3	14.3	0.0

Total terrigenous, biogenic, and "other" abundances downcore; individual grain abundances within terrigenous fraction

*Denotes second count of sample (for the twice-split samples)

[x] Denotes missing sample

Depth (mcd)	AGE (ka)	%Terr	%Bio	%Other	%Quartz	%Fe-Quartz	%Quartz-ose	%Mafic	%Volc	%Sed Frag	%Carb Frag
53.8	825.9	29.0	22.0	49.0	58.6	3.4	13.8	10.3	3.4	0.0	10.3
54.08	830.2	4.0	67.0	29.0	50.0	25.0	0.0	0.0	25.0	0.0	0.0
54.3	833.5	4.0	67.0	29.0	25.0	25.0	0.0	0.0	25.0	25.0	0.0
54.3*	833.5	3.0	69.0	28.0	66.7	0.0	0.0	0.0	0.0	33.3	0.0
54.58	837.7	0.0	98.0	2.0	0.0	0.0	0.0	0.0	0.0	0.0	0.0
54.8	841.1	0.0	29.0	71.0	0.0	0.0	0.0	0.0	0.0	0.0	0.0
55.08	845.3	2.0	63.0	35.0	50.0	0.0	0.0	0.0	50.0	0.0	0.0
55.3	848.6	0.0	44.0	56.0	0.0	0.0	0.0	0.0	0.0	0.0	0.0
55.58	852.9	24.0	33.0	43.0	50.0	8.3	29.2	0.0	8.3	4.2	0.0
55.58*	852.9	19.0	38.0	43.0	47.4	15.8	10.5	0.0	21.1	5.3	0.0

Total terrigenous, biogenic, and "other" abundances downcore. Individual grain abundances within terrigenous fraction.

*Denotes second count of sample (for the twice-split samples)

[x] Denotes missing sample